Investigation of the Redox Behavior of Ferroquine, a New Antimalarial

ARTICLE *in* MOLECULAR PHARMACEUTICS · SEPTEMBER 2008

Impact Factor: 4.38 · DOI: 10.1021/mp800007x

articles

molecular pharmaceutics

Investigation of the Redox Behavior of Ferroquine, a New Antimalarial

Natascha Chavain,[†] Hervé Vezin,[‡] Daniel Dive,[§] Nadia Touati,[‡] Jean-François Paul,[†] Eric Buisine,[‡] and Christophe Biot*,[†]

Université des Sciences et Technologies de Lille, Unité de Catalyse et Chimie du Solide—UMR CNRS 8181, Ecole Nationale Supérieure de Chimie de Lille, Bâtiment C7, B.P. 90108, 59652 Villeneuve d'Ascq cedex, France, Université des Sciences et Technologies de Lille, Laboratoire de Chimie Organique et Macromoléculaire—UMR CNRS 8009, Bâtiment C4, B.P. 90108, 59652, Villeneuve d'Ascq cedex, France, and Inserm U547, Institut Pasteur, 1 rue du Pr Calmette, B.P. 245, 59019 Lille Cedex, France

Received January 17, 2008; Revised Manuscript Received April 7, 2008; Accepted May 22, 2008

Abstract: Ferroquine (FQ or SR97193) is a unique ferrocene antimalarial drug candidate which just entered phase IIb clinical trials in autumn 2007. FQ is able to overcome the chloroquine (CQ) resistance problem, an important limit to the control of *Plasmodium falciparum,* the principal causative agent of malaria. However, as for other therapeutic agents such as chloroquine (CQ) and artemisin, its mechanism of action remains partially unknown. Most investigations have so far focused on comparing the activity of FQ to that of CQ in order to understand how the ferrocene core contributes to a stronger antiplasmodial activity. Studies have already shown that the ferrocene altered the shape, volume, lipophilicity, basicity and also electronic profile of the parent molecule and, hence, its pharmacodynamic behavior. However, few investigations have been undertaken to probe the real contribution of redox properties of the ferrocene (iron(II))/ferricinium (iron(III)) system in FQ as reported in this article. In our experimental and theoretical approach, we considered the redox profile of the ferrocene core of FQ in the specific conditions (acidic and oxidizing) of the parasitic digestive vacuole as a possible discriminating property from CQ in the antimalarial activity.

Keywords: Malaria; bioorganometallics; ferroquine; redox behavior; Fenton-like chemistry

Introduction

Ferroquine (FQ, SR97193, Figure 1) is a new antimalarial drug candidate developed by Sanofi-Aventis, currently in phase IIb of clinical trials.[1,2] This unique ferrocenic compound is able to overcome the chloroquine (CQ) resistance problem.[1,3–6] Drug resistance became effectively an impor-

* Corresponding author. Mailing address: Université des Sciences et Technologies de Lille, Unité de Catalyse et Chimie du Solide—UMR CNRS 8181, Ecole Nationale Supérieure de Chimie de Lille, Bâtiment C7, B.P. 90108, 59652 Villeneuve d'Ascq cedex, France. E-mail: christophe.biot@ensc-lille.fr. Tel: +33-(0)320434893. Fax: +33-(0)320436585.

[†] Université des Sciences et Technologies de Lille, Unité de Catalyse et Chimie du Solide—UMR CNRS 8181, Ecole Nationale Supérieure de Chimie de Lille.

[‡] Université des Sciences et Technologies de Lille, Laboratoire de Chimie Organique et Macromoléculaire—UMR CNRS 8009.

[§] Inserm U547, Institut Pasteur.

(1) Dive, D.; Biot, C. Ferrocene Conjugates of Chloroquine and other Antimalarials: the Development of Ferroquine, a New Antimalarial. *ChemMedChem.* **2007**, *3*, 383–391.

(2) http://clinicaltrialsfeeds.org/clinical-trials/show/NCT00563914.

(3) Biot, C.; Glorian, G.; Maciejewski, L.; Brocard, J.; Domarle, O.; Blampain, G.; Millet, P.; Georges, A. J.; Abessolo, H.; Dive, D.; Lebibi, J. Synthesis and antimalarial activity in vitro and in vivo of a new ferrocene-chloroquine analogue. *J. Med. Chem.* **1997**, *40*, 3715–3718.

(4) Delhaes, L.; Abessolo, H.; Biot, C.; Berry, L.; Delcourt, P.; Maciejewski, L.; Brocard, J.; Camus, D.; Dive, D. In vitro and in vivo antimalarial activity of ferrochloroquine, a ferrocenyl analogue of chloroquine against chloroquine-resistant malaria parasites. *Parasitol. Res.* **2001**, *87*, 239–244.

10.1021/mp800007x CCC: $40.75
Published on Web 06/19/2008

tant limit to the control of *Plasmodium falciparum*.[7] In this respect, FQ was revealed to be equally active on CQ-sensitive and CQ-resistant *P. falciparum* laboratory strains and field isolates.[1,4,5] Moreover FQ showed low toxicity[1] and had no cross-resistance to CQ.[8] With regard to their primary mechanism, both FQ and CQ molecules are paradoxically assumed to act by concentrating in the parasite digestive vacuole (DV), preventing thus the formation of hemozoin and finally leading to parasite death. So, the antimalarial properties of these two drugs have been compared in an effort to understand how the presence of the ferrocene core can contribute to a stronger antiplasmodial activity.[1,3,4,6,8,9]

The singularity of the ferrocene unit lies of course in its shape, volume, lipophilicity, and basicity but also electronic profile.[10] Ferrocene unsurprisingly affects the pharmacodynamic behavior of the parent molecule in which it is inserted.[9] The supposed lower affinity of FQ for the postulated transporter linked to CQ resistance has been recently attributed to these atypical physicochemical properties.[1,6] The ferrocene has also been grafted to tamoxifen, an archetypical selective estrogen receptor modulator. The hydroxyferrocifen compounds obtained revealed interestingly antiproliferative activity on breast cancer cells which are normally resistant to tamoxifen. As proposed by the authors, the ferrocene could act as an intramolecular oxidation "antenna" and facilitate the oxidative production of the putative quinone methide species responsible for the cytotoxic effect.[11,12] As also reported for a series of ferrocenyl chalcones, the ferrocene unit contributes to the antiplasmodial activity by redox cycling.[13] More hypothetically, in the acidic parasite DV the release of free heme is accompanied by the production of superoxide anion, which rapidly dismutates to H_2O_2.[14] Under such oxidizing conditions, the ferrocenyl moiety present in FQ as iron(II) could also catalyze a Fenton-like reaction, thereby yielding hydroxyl radicals. In this context, we undertook investigations to probe the contribution of the ferrocene core to the antiplasmodial activity of FQ as a possible differentiation factor from CQ. In the present article, we report our efforts to characterize the redox profile of FQ by means of cyclic voltammetry, EPR spectroscopy, spin trapping experiments, and theoretical calculations.

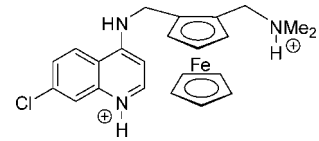

Figure 1. Chemical structure of ferroquine, diprotonated form.

Materials and Methods

Chemistry. FQ (218 mg, 0.5 mM) was diluted in dried CH_2Cl_2 (25 mL). After its complete dilution, $AgBF_4$ (98 mg, 0.5 mM) was added.[15] The reaction mixture was stirred at room temperature during 1 h. The green precipitate of [FQ][BF_4] (256 mg, 0.49 mM, 98% yield) was then filtered, and washed twice with dried diethyl ether (2 × 50 mL).

Cyclic Voltammetry. Electrochemical measurements were carried out on ferrocene, FQ (free base and dihydrochloride), CQ diphosphate and *N*,*N*-dimethylaminomethylferrocene free base (DMAF) and hydrochloride (DMAF·HCl). Ferrocene was recrystallized in ethanol−water before use, but the other compounds were used as received. DMAF·HCl was prepared in dry ether with ethanolic HCl (1 M), filtered, washed with dry ether, and dried before use. Cyclic voltammetry measurements were performed with a VoltaLab 40 system with a PGZ 301 Radiometer Analytical potentiostat. Working and auxiliary electrodes were a platinum CTV 101T and a platinum wire, respectively. The standard calomel reference electrode (SCE) was separated from the bulk of the solution by a KCl saturated solution with a glass frit. The voltammogram was recorded from a low to high potential and then reversed to the starting potential, and the scan rate in the range of 25 to 200 mV s^{-1} was measured for each compound. The electrolyte support salt was tetraethylammonium perchlorate (0.1 N). All solutions were prepared with

(5) Biot, C. Ferroquine: A New Weapon in the Fight Against Malaria. *Curr. Med. Chem.: Anti-Infect. Agents* **2004**, *3*, 135–147.
(6) Daher, W.; Biot, C.; Fandeur, T.; Jouin, H.; Pelinski, L.; Viscogliosi, E.; Fraisse, L.; Pradines, B.; Brocard, J.; Khalife, J.; Dive, D. Assessment of Plasmodium falciparum resistance to ferroquine (SSR97193) in field isolates and in W2 strain under pressure. *Malar. J.* **2006**, *5*, 11.
(7) World Health Organization. The World Health Report 2006, http://www.who.int/en.
(8) Kreidenweiss, A.; Kremsner, P. G.; Dietz, K.; Mordmüller, B. In vitro activity of ferroquine (SAR97193) is independent of chloroquine resistance in Plasmodium falciparum. *Am. J. Trop. Med. Hyg.* **2006**, *75*, 1178–1181.
(9) Biot, C.; Taramelli, D.; Forfar-Bares, I.; Maciejewski, L. A.; Boyce, M.; Nowogrocki, G.; Brocard, J. S.; Basilico, N.; Olliaro, P.; Egan, T. J. Insights into the mechanism of action of ferroquine. Relationship between physicochemical properties and antiplasmodial activity. *Mol. Pharmaceutics* **2005**, *2*, 185–193.
(10) van Staveren, D. R.; Metzler-Nolte, N. Bioorganometallic chemistry of ferrocene. *Chem. Rev.* **2004**, *104*, 5931–5985.
(11) Hillard, E.; Vessieres, A.; Thouin, L.; Jaouen, G.; Amatore, C. Ferrocene-Mediated Proton-Coupled Electron Transfer in a Series of Ferrocifen-Type Breast-Cancer Drug Candidates. *Angew. Chem., Int. Ed.* **2006**, *45*, 285–290.
(12) Schatzschneider, U.; Metzler-Nolte, N. New principles in medicinal organometallic chemistry. *Angew. Chem., Int. Ed.* **2006**, *45*, 1504–1507.
(13) Wu, X.; Tiekink, E. R. T.; Kosteski, I.; Kocherginsky, N.; Tan, A. L. C.; Khoo, S. B.; Wilairat, P.; Go, M.-L. Antiplasmodial activity of ferrocenyl chalcones: investigations into the role of ferrocene. *Eur. J. Pharm. Sci.* **2006**, *27*, 175–187.
(14) Kannan, R.; Kumar, K.; Sahal, D.; Kukreti, S.; Chauhan, V. S. Reaction of artemisinin with hemeoglobin: implications for antimalarial activity. *Biochem. J.* **2005**, *385*, 409–418.
(15) Connelly, N. G.; Geiger, W. E. Chemical Redox Agents for Organometallic Chemistry. *Chem. Rev.* **1996**, *96*, 877–910.

HPLC grade acetonitrile. The compounds (1 mM) were deoxygenated by means of a stream of dry Argon.

EPR Spectroscopy. The CW X-band EPR spectra were recorded on a Bruker ELEXYS 580-FT spectrometer. The HYSCORE measurements were carried out with the sequence $\pi/2-\tau-\pi/2-t_1-\pi-t_2-\pi/2-\tau$ echo, and a four-step phase cycle. The pulse lengths of the $\pi/2$ and π pulses in these experiments were 12 and 24 ns, respectively. All the experiments have been performed at different τ values, which have been chosen to optimize the sensitivity and to minimize the blind spot effect on the shape of the ridges. Prior to Fourier transformation of the HYSCORE data, the background decay was removed by a polynomial fit and apodized with a Hamming function. 2D FT magnitude spectra were calculated and presented as contour plots.

Spin Trapping. EPR spectra were simulated by using Winsim 2002.[16] EPR spin trapping measurements were carried out on a Bruker ELEXYS 580-FT spectrometer operating at room temperature under the following parameters: 8 mW microwave power and 1 G amplitude modulation. The sample solutions were analyzed in a flat quartz cell inserted in a standard cavity. 5,5-Dimethyl-1-pyrroline *N*-oxide (DMPO) was purchased from Fluka and used after Kugelrohr vacuum distillation to remove paramagnetic impurities. H_2O_2 aqueous solutions were freshly prepared before EPR experiments with an initial H_2O_2 solution (30%) purchased from Aldrich. A stock solution of FQ dihydrochloride (1 mM) was prepared by dissolving 12.7 mg of FQ·2HCl in 25 mL of water ACS reagent. Twenty microliters of 8 M DMPO was diluted in 1 mL of 1 mM FQ·2HCl solution before the addition of 50 μL of H_2O_2 aqueous solution. Final H_2O_2 concentrations of 1 mM and 15 mM were obtained.

Mass Spectrometry. FQ·2HCl (12.7 mg) was diluted in HPLC grade water (25 mL) with a final concentration of 1 mM. H_2O_2 stock solutions (50 mM, 500 mM, and 5 M) were prepared by diluting a commercial solution of H_2O_2 (30%) in HPLC grade water. Samples were then prepared by adding 20 μL of H_2O_2 stock solution to 1 mL of FQ solution. The final concentrations of H_2O_2 were 1 mM, 10 mM and 100 mM. Reactions between FQ and H_2O_2 were monitored up to 31 h. 0.5 μL of reaction mixture was spotted after 0, 0.5, 1, 5, 6, 7, 24 and 31 h on a MALDI target with 1 μL of 2′,4′,6′-trihydroxyacetophenone (THAP)/ammonium citrate 9/1 v/v matrix (THAP 10 mg/mL in H_2O/acetonitrile, v/v, and ammonium citrate 50 mg/mL in water) using the dried droplet method. Matrix-assisted laser desorption ionization/time-of-flight (MALDI-TOF) mass spectra were acquired using a Voyager DE-STR instrument (Applied Biosystems) equipped with a nitrogen laser operating at a wavelength of 337 nm in reflector positive ion mode. 100−125 laser shots were accumulated for each spectrum.

Computational Details. All calculations were performed with the Amsterdam Density Functional (ADF) program.[17,18] Molecular orbitals (MOs) were expanded using a large triple-ζ (TZP) basis set,[19] augmented by one set of polarization functions. Scalar relativistic corrections were included self-consistently using the zeroth order regular approximation (ZORA).[20] Geometries were optimized using the Perdew−Wang 1991 (PW91) correlation functionals[21] in singlet, triplet and quintet spin states for iron(II) and in doublet, quartet and sextet spin states for iron(III).

Results and Discussion

Chemistry. The "ferriquinium salt" [FQ][BF_4] was prepared in good yield by chemical oxidation of FQ with $AgBF_4$ in dichloromethane (DCM) at room temperature. [FQ][BF_4] is green in color and is stable as a solid. $AgBF_4$ is among the most widely used one-electron oxidants. As the formal potential of Ag^+/Ag is solvent dependent, three different solvents were tried: acetonitrile ($E^{\circ\prime} = 0.04$ V), acetone ($E^{\circ\prime} = 0.18$ V) and DCM ($E^{\circ\prime} = 0.65$ V).[15] Whereas all solutions turned green when adding the silver (I) ion, only the solid isolated from DCM was pure [FQ][BF_4]. The other two contained a mixture of iron(II) and iron(III) as revealed by EPR spectroscopy (data not shown). This indicates that FQ is relatively difficult to oxidize as confirmed by the CV studies (see below).

In aqueous solution, the paramagnetic FQ^+ cation rapidly evolves toward the diamagnetic neutral FQ, as evidenced by NMR and EPR studies. To fully characterize the ferriquinium salt, solid EPR spectra were recorded.

Cyclic Voltammetry. Table 1 lists the changes in electrode potential (ΔE_p) and half-wave potential $E_{1/2}$ of the tested compounds as the difference between the oxidation and reduction potential, ΔE_p, reflects the reversibility of the reaction. With regard to $E_{1/2}$, a large value of this redox parameter indicates resistance to electron loss.

(16) Duling, D. R. Simulation of Multiple Isotropic Spin Trap EPR Spectra. *J. Magn. Reson., Ser. B* **1994**, *104*, 105–110.

(17) Baerends, E. J.; Autschbach, J.; Bérces, A.; Bo, C.; de Boeij, P. L.; Boerrigter, P. M.; Cavallo, L.; Chong, D. P.; Deng, L.; Dickson, R. M.; Ellis, D. E.; Fan, L.; Fischer, T. H.; Fonseca Guerra, C.; van Gisbergen, S. J. A.; Groeneveld, J. A.; Gritsenko, O. V.; Grüning, M.; Harris, F. E.; van den Hoek, P.; Jacobsen, H.; van Kessel, G.; Kootstra, F.; van Lenthe, E.; McCormack, D. A.; Michalak, A.; Osinga, V. P.; Patchkovskii, S.; Philipsen, P. H. T.; Post, D.; Pye, C. C.; Ravenek, W.; Ros, P.; Schipper, P. R. T.; Schreckenbach, G.; Snijders, J. G.; Solà, M.; Swart, M.; Swerhone, D.; te Velde, G.; Vernooijs, P.; Versluis, L.; Visser, O.; Wang, F.; van Wezenbeek, E.; Wiesenekker, G.; Wolff, S. K.; Woo, T. K.; Yakovlev, A. L.; Ziegler, T. SCM: Amsterdam, 2005.

(18) te Velde, G.; Bickelhaupt, F. M.; Baerends, E. J.; Fonseca Guerra, C.; van Gisbergen, S. J. A.; Snijders, J. G.; Ziegler, T. Chemistry with ADF. *J. Comput. Chem.* **2001**, *22*, 931–967.

(19) van Lenthe, E.; Baerends, E. J. Optimized Slater-type basis sets for the elements 1−118. *J. Comput. Chem.* **2003**, *24*, 1142–1155.

(20) van Lenthe, E.; Baerends, E. J.; Snijders, J. G. Relativistic regular two-component Hamiltonians. *J. Chem. Phys.* **1993**, *99*, 4597–4610.

(21) Perdew, J. P.; Wang, Y. Accurate and simple analytic representation of the electron-gas correlation energy. *Phys. Rev. B.* **1992**, *45*, 13244–13249.

Table 1. Reversible Half-Wave Potentials $E_{1/2}$ and Changes in Electrode Potential ΔE_p Values of Tested Ferrocenyl Compounds (1 mM, 100 mV/s)

compound	$E_{1/2}$ (mV)	ΔE_p (mV)
ferrocene	393.5	62.1
DMAF	387.5	65.0
DMAF·HCl	551.0	63.0
FQ	461.5	63.0
FQ·2HCl	651.7	75.5

The ΔE_p values obtained for all the compounds studied were in the range 62.0−75.5 mV, indicating a reversible single electron transfer mechanism. A linear dependence was moreover observed between the electrode current required for the oxidation/reduction reaction of each compound and the square root of scan rate. These results provide strong support for the reversibility of the electron transfer process.

In the potential range investigated, all ferrocenyl compounds showed the presence of one diffusion-controlled redox couple (Figure 2). In comparison with CQ which is totally devoid of redox properties, the electron transfer observed for FQ and other ferrocenyl compounds arises specifically from the iron core of the ferrocene moiety as confirmed by the DFT calculations. The reference $E_{1/2}$ value measured versus SCE for a single ferrocene unit is 393.5 mV. This value is very close to the 400 mV previously measured for ferrocene with platinum wires as working and auxiliary electrode versus SCE.[22] Markedly, except for the DMAF molecule, this value is the lowest, thus suggesting that all other ferrocenyl derivatives in which ferrocene is substituted exhibit higher resistance to electron loss, e.g. oxidation mechanisms take place at higher potential. In this respect, the propensity for electron loss from ferrocene was known to be strongly influenced by the type of substituents attached to its cyclopentadienyl rings.[23–28] The value of $E_{1/2}$ was 387.5 mV for DMAF, close to the ferrocene standard half-potential, whereas it was significantly increased to 461.5 mV for FQ. Furthermore, when these two species became protonated, their resistance to electron loss was exacerbated. The values of $E_{1/2}$ for DMAF·HCl and FQ·2HCl increased significantly to 551.0 and 651.0 mV respectively. These higher $E_{1/2}$ values result from the strong electron withdrawing effect exerted by the positive charges of protonated side chains. In the case of FQ, this withdrawing effect is due not only to the positively charged alkylamino side chain of ferrocene as in DMAF·HCl but also to the protonated quinoline ring. Hence, diprotonated FQ gave the highest $E_{1/2}$ value compared to the other compounds.

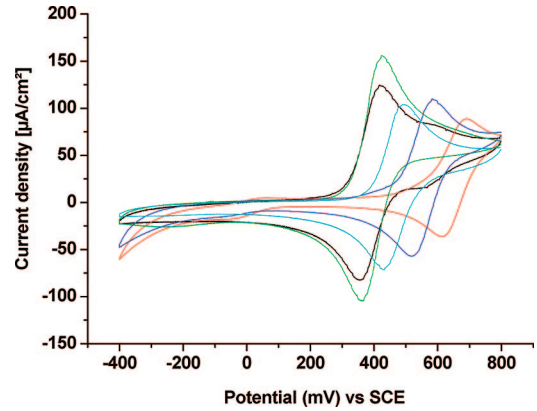

Figure 2. Cyclic voltammograms of ferrocene (green line), DMAF (black line), DMAF·HCl (dark blue line), FQ (blue line), and FQ·2HCl (red line) recorded at 1 mM in acetonitrile (0.1 M TEAP) and at a scan rate of 100 mV/s.

EPR Experiments. The CW-EPR spectrum of paramagnetic ferriquinium salt [FQ][BF_4] presented a broad line of 150 G centered at $g = 2.01$ as previously described.[29] These signals arose from the iron(III) in its doublet spin state ($S = 1/2$). These results are consistent with theoretical calculations for which the doublet state for iron(III) is predicted as the most stable (see below).

Additional pulse EPR experiments have been performed using two-dimensional four-pulse ESEEM (HYSCORE), which is a very useful sequence to measure the superhyperfine interactions between the nuclei environment coupled to the electron spin of iron(III) (Figure 3). The spectrum revealed weak coupling only in the (+,+) quadrant with essentially proton pattern cross peak ridge. These cross peaks coordinated 20.2−9.8 and 9.8−20.2 MHz and were centered at 15.2 MHz along the diagonal $\omega_1 = \omega_2$. These result from a vertical shift of 0.7 MHz from the proton Larmor frequency of 14.5 MHz. Such coupling values arise from the dipolar part of hyperfine tensor of the distributed protons of the cyclopentadienyl ring. Additional features were also observed

(22) Lemoine, P.; Gross, M.; Braunstein, P.; Mathey, F.; Deschamps, B.; Nelson, J. H. Electrochemistry of Phosphaferrocenes. 1. Comparison of the redox properties of ferrocene diphosphaferrocene, 3,4-dimethyl-1-phosphaferrocene, and 3,3′,4,4′-tetramethyl-1,1′-diphosphaferrocene. *Organometallics* **1984**, *3*, 1303–1307.

(23) Zanello, P.; Cinquantini, A.; Mangani, S.; Opromolla, G.; Pardi, L.; Janiak, C.; Rausch, M. D. The redox behaviour of ferrocene derivatives: VI. Benzylferrocenes. The crystal structure of decabenzylferrocenium tetrafluoroborate. *J. Organomet. Chem.* **1994**, *471*, 171–177.

(24) Martinez, R.; Tiripicchio, A. Structure of ferrocenium hexafluorophosphate. *Acta Crystallogr.* **1990**, *C46*, 202–205.

(25) Pickardt, J.; Schumann, H.; Mohtachemi, R. Structure of decamethylferrocenium tribromide. *Acta Crystallogr.* **1990**, *C46*, 39–41.

(26) Rausch, M. D.; Tsai, W. M.; Chambers, J. W.; Rogers, R. D.; Alt, H. G. Synthetic and x-ray structural studies on pentabenzylcyclopentadienyl derivatives of manganese, rhenium, and iron. *Organometallics* **1989**, *8*, 816–821.

(27) Seiler, P.; Dunitz, J. D. A new interpretation of the disordered crystal structure of ferrocene. *Acta Crystallogr.* **1979**, *B35*, 1068–1074.

(28) Freyberg, D. P.; Robbins, J. L.; Raymond, K. N.; Smart, J. C. Crystal and molecular structures of decamethylmanganocene and decamethylferrocene. Static Jahn-Teller distortion in a metallocene. *J. Am. Chem. Soc.* **1979**, *101*, 892–897.

(29) Prins, R.; Reinders, F. J. Electron spin resonance of the cation of ferrocene. *J. Am. Chem. Soc.* **1969**, *91*, 4929–4931.

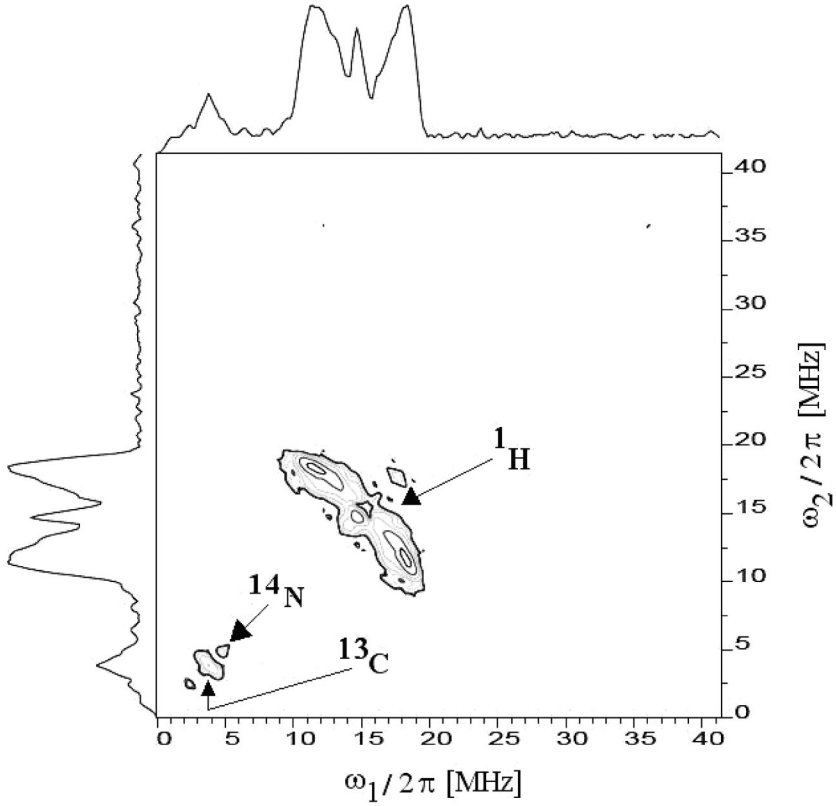

Figure 3. 2D HYSCORE spectrum recorded at 4 K for $\tau = 196$ ns.

with ^{13}C Larmor nuclear frequency at 3.7 MHz and double quantum transition of ^{14}N. Both coupling constants were too small to be measured but indicated that a fraction of spin density was delocalized on the nitrogen atom.

DFT Calculations. Density functional theory (DFT) calculations were performed on ferrocene, neutral and diprotonated FQ molecules. For FQ, crystal structures were used as starting point.[9] For diprotonated FQ, the chloride ion bridging the nitrogen atom of the dimethylaminomethyl side chain and the nitrogen atom at position 4 were kept for calculations. Molecular geometries have been fully optimized for both the iron(II) and iron(III) species. The optimized structures of diprotonated FQ are given in the Supporting Information.

First, energy calculations indicated that the lowest energy spin states were always the singlet (spin multiplicity $S = 0$) for the iron(II) and the doublet ($S = 1/2$) for the iron(III). For iron(II) ferrocene and neutral FQ molecules, the energy difference between their singlet and triplet spin states was around 33 kcal/mol. For iron(III) molecules, the energy difference between their doublet and quartet spin states were around 26 and 20 kcal/mol for ferrocene and neutral FQ respectively. The energies of formation for iron(III) doublet states from their iron(II) singlet states have been also estimated and revealed to be in good agreement with the variation trends in $E_{1/2}$ potential values as obtained by cyclic voltammetry. The energy differences between the iron(III) and iron(II) electronic ground states were estimated to be 152, 160 and 209 kcal/mol for ferrocene, neutral FQ and diprotonated FQ respectively. Diprotonated FQ is here clearly confirmed as the most difficult to oxidize as evidenced by cyclic votammetry due to its highest $E_{1/2}$ potential value.

The calculation of the spin population on the iron(III) of diprotonated FQ gave a value of 1.09 electrons occupying mainly the d shell. This result is coherent with the increased distances between the iron(III) atom and the carbon atoms of the cyclopentadienyl rings in comparison to those observed with iron(II). Similar trends were observed for isolated ferrocene. The overlap population between the iron atom and all the hydrogen atoms of the cyclopentadienyl rings were almost equivalent. The coupling with these nuclear spins were similar and cannot be individualized. Indeed, computation of anisotropic hyperfine tensor showed a small a_{iso} Fermi contact term value of 0.45 MHz whereas the dipolar components were in the range of 2 to 5 MHz. Such values were consistent with the proton pattern observed in the HYSCORE spectrum.

Spin Trapping. Under oxidizing conditions, iron(II) either free or present in ferrocene[11] has been reported for its ability to give a Fenton-like reaction, thereby yielding hydroxyl radicals ($HO^{\bullet}$):

$$Fe^{2+} + H_2O_2 \rightarrow Fe^{3+} + HO^- + HO^{\bullet}$$

Logically, we set out to test whether the ferrocene core present in FQ could also catalyze this kind of reaction:

$$FQ(II) + H_2O_2 \rightarrow FQ(III) + HO^- + HO^{\bullet}$$

In this regard, EPR spin trapping experiments were carried out. The spin trap agent used to observe the formation of

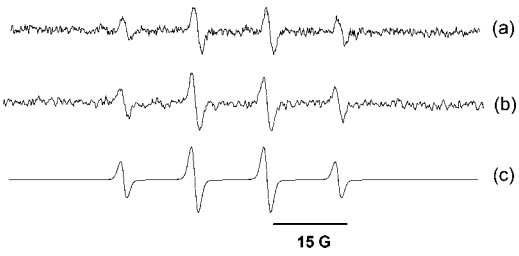

Figure 4. EPR spin trapping spectra at room temperature: (a) FQ·2HCl (1 mM), H_2O_2 (1 mM); (b) FQ·2HCl (1 mM), H_2O_2 (15 mM); (c) simulated spectrum with hyperfine coupling constants $a_H = a_N = 14.9$ G. The final DMPO concentration was 0.16 M.

hydroxyl radicals was DMPO. Oxidizing conditions were induced by adding H_2O_2 solutions at two different concentrations, 1 mM and 15 mM respectively. The latter is supposed to be the concentration at which H_2O_2 is found in the food vacuole of the parasite.[14] In this respect, the pH in the food vacuole of the parasite being acidic, around 5, only the diprotonated FQ species was tested for its ability to form radicals.

The EPR spectra given in Figure 4 displayed a typical quartet with an intensity ratio of 1:2:2:1 and hyperfine splitting coupling constants, $a_H = a_N = 14.9$ G. These spectroscopic results unambiguously evidenced the formation of hydroxyl radical spin adduct DMPO−OH$^\bullet$.

The HO$^\bullet$ radicals formed by FQ·2HCl during the Fenton reaction were quantified by double integration of EPR spectra. 2,2,6,6-Tetramethylpiperidinyl-1-oxyl (TEMPO) was used as intensity reference at a concentration of 0.1 mM in methanol. A hydroxyl production of 0.47 μM and of 2.55 μM was then measured for FQ·2HCl in the presence of 1 mM and 15 mM H_2O_2, respectively. These results are clearly in accordance with the low efficiency of oxidation of diprotonated FQ, as evidenced by cyclic voltammetry and also predicted by theoretical calculations.

Stability of Ferroquine in the Presence of H_2O_2. The stability of FQ was investigated in oxidizing conditions mimicking the parasite food vacuole (acidic pH and micromolar concentrations in H_2O_2). During the erythrocytic phase of the malaria parasite, the formation of hydrogen peroxide only occurs during stages when the parasite is degrading internalized red blood cell content. Indeed, the degradation of hemoglobin in the food vacuole is accompanied by the release of free heme, and then by production of superoxide anion, which dismutates into H_2O_2.

MALDI-TOF mass spectrometry has been used to investigate the stability of FQ in water in the presence of H_2O_2. The FQ degradation products were assessed at different concentrations of H_2O_2: 1 mM, 10 mM and 100 mM. Final solutions of 1 mM FQ with H_2O_2 in water were spotted after different reaction times.

FQ, the initial chemical structure,was clearly detected on the MALDI-TOF spectrum at *m*/*z* 434 (^{35}Cl) and 436 (^{37}Cl) with an isotopic distribution corresponding to the presence of Fe and Cl (Figure 5). Analyses of MS data showed then that oxidation of FQ occurred but was detected only after

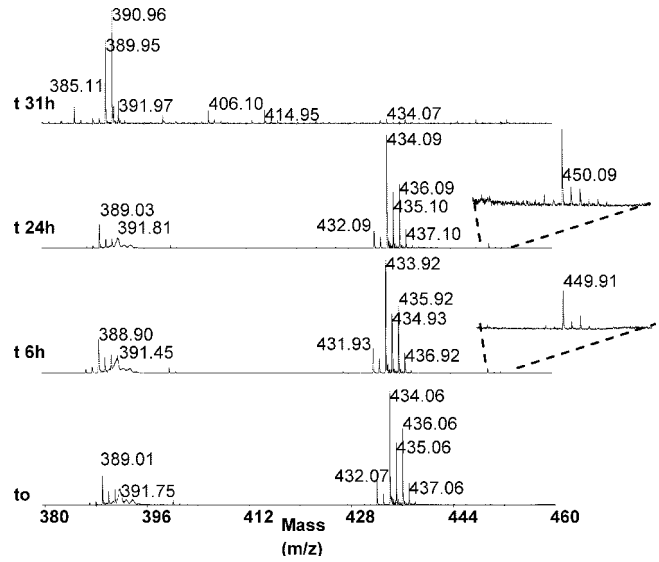

Figure 5. MALDI-TOF spectrum of the FQ solution in presence of 100 equiv of H_2O_2 at t_0 and after 6, 24 and 31 h.

6 h with an H_2O_2 concentration of 100 mM or only after 31 h with a H_2O_2 concentration of 10 mM. This slow oxidation led to the formation of 7-chloro-4-(2-(*N*,*N*-dimethylaminomethyl) ferrocenylmethylaminoquinoline oxide unambiguously detected at *m*/*z* 449 (^{35}Cl) and 451 (^{37}Cl) and already reported as a minor metabolite of FQ (Met D).[6] Finally, to observe a complete disappearance of the MS peak attributed to FQ, it was necessary to incubate FQ during 31 h at the high H_2O_2 concentration of 100 mM. The degradation of FQ was linked with the detection of the fragment at *m*/*z* 389 (^{35}Cl) and 391 (^{37}Cl) resulting from the loss of the dimethylamino group (Figure 5).

Redox Activity of FQ in Chemical Conditions of *Plasmodium falciparum* Digestive Vacuole: Implications for Antimalarial Activity. Under oxidizing conditions mimicking the parasite DV, FQ shows a reversible one-electron redox reaction. This leads to the formation of ferriquinium and generation of hydroxyl radicals, with kinetics which are relevant for an antimalarial activity on *P. falciparum*. CQ has been shown to induce reactive oxygen species (ROS) production in astroglial cells via a signaling pathway involving NFκ-B.[30,31] In the red blood cell devoid of a nucleus, such a pathway cannot occur. The present spin trapping experiments demonstrate that CQ is not able to produce OH$^\bullet$ radicals by itself in the presence of hydrogen peroxide at the pH of the parasite DV. On the contrary, using the same experimental conditions, hydroxyl radicals are produced by FQ at micromolar concentration. Nevertheless,

(30) Park, J.; Kwon, D.; Choi, C.; Oh, J.-W.; Benveniste, E. N. Chloroquine induces activation of nuclear factor-B and subsequent expression of pro-inflammatory cytokines by human astroglial cells. *J. Neurochem.* **2003**, *84*, 1266–1274.

(31) Park, J.; Choi, K.; Jeong, E.; Kwon, D.; Benveniste, E. N.; Choi, C. Reactive oxygen species mediate chloroquine-induced expression of chemokines by human astroglial cells. *Glia* **2004**, *47*, 9–20.

this weak production of hydroxyl radicals should be sufficient to induce significant damage, due to the very high reactivity of these radicals.

According to our results, FQ might thus strike the parasite not only *via* direct inhibition of hemozoin formation but also by production of lethal hydroxyl radicals. Indeed, these radicals are known to be particularly aggressive toward unsaturated fatty acids present in membrane phospholipids and to promote an extensive chain reaction of their peroxidation products.[32] The parasite DV contains lipid bodies and membrane complexes[33,34] whose lipid/aqueous interfaces were suspected to promote a rapid sequestration of heme into hemozoin.[35] These interfaces are also thought to be a site of concentration of FQ which is much more lipophilic than CQ.[1,9] The alteration or the destruction of these structures should then influence heme detoxification process(es) and could result in a complementary harmful effect on the parasite. Since the toxic action of hydroxyl radicals occurred very quickly, FQ may induce severe damages to the parasite and amplify inhibition of hemozoin formation, before intervention of resistance mechanisms. Hence, FQ could remain active on CQ resistant parasites.

Further experiments will be necessary to provide answers to these hypotheses. Hydroxyl radical attack of fatty acids results in the production of byproduct such as malonaldehyde and hydroxynonenal which can be titrated.[32,36] Malonaldehyde reacts with free NH_2 functions of basic amino acids, resulting in amino−imino−propene bridges which can be recognized by specific antibodies[37,38] in ELISA, Western or dot blots, and by indirect immunofluorescence examination of cells.[39] Comparison of CQ and FQ action on parasites would provide complementary information on the relevance of the complementary ROS mechanism we propose here for FQ.

Conclusion

If the major contribution to the activity of the new antimalarial FQ should maintain its effects upon heme catabolism, by binding to hematin and thus preventing its aggregation into hemozoin,[1,9] another contribution could also arise from its redox properties. Indeed, the results described in this article reveal, that owing to its ferrocene moiety, FQ is able to generate small amounts of hydroxyl radicals from H_2O_2 *via* a Fenton-like reaction. Upon such specific oxidizing conditions (parasitic DV), this production of ROS appears not sufficient to affect the stability of FQ. On the other hand, it should be sufficient to promote significant damage on membranes of the parasite DV, also suspected to be a site of concentration of FQ. By specific *in situ* production of hydroxyl radicals, FQ might induce severe damage to the parasite before intervention of resistance mechanisms.

Acknowledgment. The authors thank Adeline Page for her generous assistance with the MS spectroscopy. A BDI fellowship from CNRS and Region Nord-Pas-de-Calais to N.C. is gratefully acknowledged. Clément Roux is acknowledged for proof-reading the manuscript.

Supporting Information Available: Cartesian coordinates of the diprotonated ferroquine (doublet spin state) whose geometry is optimized at PW91/TZP, and Cartesian coordinates of the diprotonated ferriquinium (singlet spin state) whose geometry is optimized at PW91/TZP. This material is available free of charge via the Internet at http://pubs.acs.org.

MP800007X

(32) Cherubini, A.; Ruggiero, C.; Polidori, M. C.; Mecocci, P. Potential markers of oxidative stress in stroke. *Free Radical Biol. Med.* **2005**, *39*, 841–852.

(33) Jackson, K. E.; Klonis, N.; Ferguson, D. J.; Adisa, A.; Dogovski, C.; Tilley, L. Food vacuole-associated lipid bodies and heterogeneous lipid environments in the malaria parasite, *Plasmodium falciparum*. *Mol. Microbiol.* **2004**, *54*, 109–122.

(34) Pisciotta, J. M.; Coppens, I.; Tripathi, A. K.; Scholl, P. F.; Shuman, J; Bajad, S; Shulaev, V; Sullivan, D. J., Jr. The role of neutral lipid nanospheres in Plasmodium falciparum heme crystallization. *Biochem. J.* **2007**, *402*, 197–204.

(35) Egan, T. J.; Chen, J. Y.; de Villiers, K. A.; Mabotha, T. E.; Naidoo, K. J.; Ncokazi, K. K.; Langford, S. J.; McNaughton, D.; Pandiancherri, S.; Wood, B. R. Hemeozoin (beta-hemeatin) biomineralization occurs by self-assembly near the lipid/water interface. *FEBS Lett.* **2006**, *580*, 5105–5110.

(36) Meagher, E. A.; FitzGerald, G. A. Indices of lipid peroxidation in vivo: strengths and limitations. *Free Radical Biol. Med.* **2000**, *28*, 1745–1750.

(37) Petit, E.; Chancerelle, Y.; Dumont, E.; Divoux, D.; Kergonou, F.; Nouvelot, A. Polyclonal antibodies against malondialdehyde-modified proteins: characterization and application in study of in vitro lipid peroxidation of cellular membranes. *Biochem. Mol. Biol. Int.* **1995**, *36*, 355–364.

(38) Chancerelle, Y.; Mathieu, J.; Kergonou, J. F. Antibodies against malondialdehyde-modified proteins. Induction and ELISA measurement of specific antibodies. *Methods Mol. Biol.* **1998**, *108*, 111–118.

(39) Storme, L.; Zerimech, F.; Riou, Y.; Martin-Ponthieu, A.; Devisme, L.; Slomianny, C.; Klosowski, S.; Dewailly, E.; Cneude, F.; Zandecki, M.; Dupuis, B.; Lequien, P. Inhaled nitric oxide neither alters oxidative stress parameters nor induces lung inflammation in premature lambs with moderate hyaline membrane disease. *Biol. Neonate* **1998**, *73*, 172–181.